Faraday Discussions

Cite this: *Faraday Discuss.*, 2018, **207**, 409

PAPER

Exploring oligomeric state of the serotonin$_{1A}$ receptor utilizing photobleaching image correlation spectroscopy: implications for receptor function

Hirak Chakraborty, [ab] Md. Jafurulla, [a] Andrew H. A. Clayton *[c] and Amitabha Chattopadhyay *[a]

Received 31st August 2017, Accepted 6th October 2017
DOI: 10.1039/c7fd00192d

The oligomerization of G protein-coupled receptors (GPCRs) represents an important process in GPCR function and drug discovery. We have addressed cholesterol-dependent oligomerization state of the serotonin$_{1A}$ receptor, a representative GPCR and an important drug target, utilizing photobleaching image correlation spectroscopy (pbICS). pbICS allows determination of oligomeric state of membrane receptors since change in cluster density upon photobleaching is dependent on the oligomeric state. Our results show that oligomeric state of the serotonin$_{1A}$ receptor is modulated by cell membrane cholesterol and a trimeric population of the receptor prevails in control (normal) cholesterol conditions. Interestingly, upon lowering membrane cholesterol, the predominant oligomeric population of the receptor changes to dimers. This is associated with an increase in specific ligand binding activity of the receptor, thereby implying a crucial role of receptor dimers in ligand binding activity. Upon cholesterol replenishment, the distribution of receptor oligomers is further changed such that the trimers become the major population, with a concomitant restoration of ligand binding activity to the control level. These results demonstrate the utility of pbICS in monitoring oligomeric states of membrane receptors in general, and the cholesterol-dependent oligomeric state of the serotonin$_{1A}$ receptor in particular. We envision that functional correlates of oligomeric states of GPCRs could provide better understanding of GPCR function in health and disease, and help design better therapeutic strategies.

[a]*CSIR-Centre for Cellular and Molecular Biology, Hyderabad 500 007, India. E-mail: amit@ccmb.res.in*
[b]*School of Chemistry, Sambalpur University, Jyoti Vihar, Burla, Odisha 768 019, India*
[c]*Centre for Microphotonics, Faculty of Science, Engineering and Technology, Swinburne University of Technology, Hawthorn, Victoria 3122, Australia. E-mail: aclayton@swin.edu.au*

Introduction

G protein-coupled receptors (GPCRs) are a family of seven transmembrane domain proteins that act as signaling hubs and transfer information from outside the cell to the cellular interior.[1–3] GPCRs facilitate a large number of physiological responses to a variety of stimuli, thereby mediating multiple cellular processes which include neurotransmission, cellular metabolism, inflammatory and immune responses, secretion, cellular differentiation and growth. As a result, GPCRs serve as major (~50%) drug targets in all clinical areas.[4,5] Work from a number of laboratories has shown that membrane lipids, particularly cholesterol and sphingolipids, have a crucial role in the function of GPCRs.[6–11] An active and exciting area in GPCR biology is the oligomerization of GPCRs and its role in receptor function.[12–16] GPCR oligomerization is believed to increase the cross-talk between receptors and their downstream signaling, which results in efficient and controlled signal transduction.[17–19] Interestingly, membrane lipids have been shown to modulate oligomerization of GPCRs.[20–27]

GPCR oligomerization has been studied using a variety of approaches. Yet, monitoring receptor oligomerization under varying conditions has proved to be challenging.[19,28–30] Due to the challenges involved in monitoring GPCR oligomers in complex and dynamic cell membranes, a number of biochemical, biophysical and simulation-based approaches have been used.[30,31] Image correlation spectroscopy (ICS) provides a useful approach for exploring the oligomerization state of membrane receptors.[32–36] ICS offers an advantage over conventional fluorescence correlation spectroscopy (FCS) as it measures spatial correlation instead of temporal correlation, which is measured in FCS. Due to the slow diffusion of membrane proteins, FCS is not suitable for analyzing receptor distribution in cell membranes.[37] ICS measures the fluctuation of fluorescence intensity in space and the spatial autocorrelation function provides the cluster density. The cluster density changes upon photobleaching of the fluorophore. In photobleaching ICS (pbICS), the cluster density is measured as a function of remaining fluorescence and the relation between cluster density and remaining fluorescence depends on the oligomeric state of the protein.[35] The average cluster density is directly proportional to remaining fluorescence (subsequent to photobleaching) for monomers, but is a nonlinear function for higher order oligomers (dimers and above). pbICS has therefore proved to be a convenient approach for determining aggregation states of membrane receptors in intact cells.[35]

The serotonin$_{1A}$ receptor is an important neurotransmitter receptor and belongs to the GPCR family. It is implicated in behavior, learning, development and cognition,[38,39] and serves as a crucial drug target for neuropsychiatric disorders and cancer.[40,41] We have previously shown that membrane cholesterol and sphingolipids play an important role in the function[6,7,9,10] and oligomerization[20–23] of the serotonin$_{1A}$ receptor. In this work, we have explored the cholesterol-dependent oligomerization state of the serotonin$_{1A}$ receptor by performing pbICS measurements on Chinese Hamster Ovary (CHO) cells stably expressing the enhanced yellow fluorescent protein (EYFP)-tagged serotonin$_{1A}$ receptor (5-HT$_{1A}$R-EYFP). Our results show that serotonin$_{1A}$ receptors exhibit a heterogeneous distribution of monomers, dimers and trimers in control cells. Upon depletion of membrane cholesterol, the distribution is changed such that the population of receptor dimers is increased. Further correlation of ligand binding

activity with the oligomeric state of the receptor reveals that the dimeric receptor could be most active in terms of ligand binding.

Experimental

Materials

$MgCl_2$, $CaCl_2$, cholesterol, penicillin, streptomycin, gentamicin sulfate, serotonin and methyl-β-cyclodextrin (MβCD) were obtained from Sigma Chemical Co. (St. Louis, MO). [^{3}H]8-OH-DPAT (specific activity 141.4 Ci mmol^{-1}) was purchased from MP Biomedicals (Santa Ana, CA). Dulbecco's modified Eagle's medium (DMEM)/F-12 (nutrient mixture F-12, Ham; 1 : 1), fetal calf serum, and geneticin (G418) were obtained from Invitrogen Life Technologies (Carlsbad, CA). Bicinchoninic acid (BCA) assay reagent was purchased from Pierce (Rockford, IL). GF/B glass microfiber filters were from Whatman International (Kent, UK). All other chemicals used were of highest purity. Water was purified through a Millipore (Bedford, MA) Milli-Q system and used throughout.

Cells and cell culture

CHO-K1 cells stably expressing the serotonin$_{1A}$ receptor tagged to EYFP (~10^5 receptors per cell; abbreviated as CHO-5-HT$_{1A}$R-EYFP) were used.[42] Cells were grown in DMEM/F-12 (1 : 1) supplemented with 2.4 g l^{-1} of sodium bicarbonate, 10% fetal calf serum, 60 μg ml^{-1} penicillin, 50 μg ml^{-1} streptomycin, and 50 μg ml^{-1} gentamicin sulfate in a humidified atmosphere with 5% CO_2 at 37 °C. CHO-5-HT$_{1A}$R-EYFP cells were maintained in presence of 300 μg ml^{-1} geneticin.

Treatment of cells

Cells plated at a density of 2×10^4 on cover slips or 5×10^5 in 100 mm Petri dishes were grown for 3 days followed by incubation in serum-free D-MEM/F-12 (1 : 1) medium for 3 h. Cholesterol depletion was carried out by treating cells with 10 mM MβCD in serum-free medium at 37 °C for 30 min. For replenishment of cellular cholesterol, cholesterol-depleted cells were incubated with 1 mM cholesterol as a pre-formed MβCD-cholesterol (10 : 1, mol/mol) complex (prepared as described earlier[43]) at 37 °C for 10 min. Cells were then washed with PBS (containing 1 mM $CaCl_2$ and 0.5 mM $MgCl_2$) and fixed using 4% (v/v) formaldehyde solution and used for microscopy. For measuring agonist binding activity of the serotonin$_{1A}$ receptor, cell membranes were prepared as described earlier.[44] Protein concentration in isolated membranes was assayed using BCA reagent.[45] All experiments were performed at room temperature (~23 °C).

Estimation of cholesterol

Cholesterol content in cell membranes was estimated using Amplex Red cholesterol assay kit.[46]

Radioligand binding assay

Receptor binding assays with the radiolabeled agonist 8-hydroxy-2(di-*N*-propylamino)tetralin ([^{3}H]8-OH-DPAT), at a final concentration of 1 nM, were carried out as described previously.[44]

pbICS experiments

pbICS measurements of control and cholesterol-modulated CHO-5-HT_{1A}R-EYFP cells were carried out with an inverted Zeiss LSM 510 Meta confocal laser scanning microsope (Jena, Germany) with a 63×, 1.4 NA oil-immersion objective using the 514 nm line of an argon laser as the excitation source. Fluorescence emission was collected using a Zeiss LSM Meta detector over an emission range of 520–555 nm. Typically, 128 × 128 pixel regions of interest (ROIs) on the upper cell surfaces were selected for ICS analysis. ROIs were auto-correlated using the Fourier Transformed Math option in ImageJ (National Institutes of Health, Bethesda), normalized by the number of pixels and average intensity squared, and corrected for background intensity. Data were fitted to a Gaussian-plus-offset function.[36]

Results

Analysis of pbICS results in terms of receptor oligomeric state

The amplitude of the autocorrelation function $g(0)$ and the full width at half maximum (r) are related to the cluster density (CD, number of clusters per square micron) by the equation:[36]

$$\mathrm{CD} = 1/[g(0)\pi r^2] \tag{1}$$

The above method was used to calculate autocorrelation parameters in frames in a stack that was collected as a function of photobleaching. For each image in the acquired bleaching time series, the fractional remaining fluorescence after bleaching ($p(t)$) was computed as

$$p(t) = [I(t) - I_\mathrm{b}(t)]/[I(t=0) - I_\mathrm{b}(t=0)] \tag{2}$$

where I and I_b are intensities of the ROI and background, respectively. The plot of cluster density as a function of fractional remaining fluorescence (p) can be fitted for homogenous distribution of monomers, dimers, trimers and j-mers. The expression of CD as a function of p is given by:[35]

$$\text{Monomer: } \mathrm{CD}(p) = c_1 p \tag{3}$$

$$\text{Dimer}: \quad \mathrm{CD}(p) = \frac{c_2}{\left(\frac{1}{2p}\right) + \left(\frac{1}{2}\right)} \tag{4}$$

$$\text{Trimer}: \quad \mathrm{CD}(p) = \frac{c_3}{\left(\frac{1}{3p}\right) + \left(\frac{2}{3}\right)} \tag{5}$$

$$j\text{-mer} = \frac{c_j}{\left(\frac{1}{jp}\right) + \left(\frac{j-1}{j}\right)} \tag{6}$$

where c_j is the mean concentration of the j^{th} species. However, the plot of experimentally determined cluster density as a function of fractional remaining fluorescence does not fit to any homogeneous model. We therefore analyzed all

data in a monomer–dimer–trimer model, where we varied the fractional abundance (α_i) of monomer, dimer and trimer using the following equation:

$$g(0,p) = \frac{\alpha_1}{\mathrm{CD}(p)_{\mathrm{monomer}}} + \frac{\alpha_2}{\mathrm{CD}(p)_{\mathrm{dimer}}} + \frac{\alpha_3}{\mathrm{CD}(p)_{\mathrm{trimer}}} \quad (7)$$

where $g(0,p)$ is the autocorrelation function at zero lag as a function of photobleaching and $\alpha_1 + \alpha_2 + \alpha_3 = 1$. The fractional components are proportional to the square of the intensity contributions, *e.g.*, $(\alpha_1 = \langle i_1\rangle^2/\langle i_T\rangle^2)$, where $\langle i_1\rangle$ is the average intensity from monomer population and $\langle i_T\rangle$ is the sum of the intensity contributions from monomer, dimer and trimer. The fitting of the plot of cluster density as a function of fractional remaining fluorescence in a monomer–dimer–trimer model yielded the fractional components of monomer, dimer and trimer population of receptors in the cell membrane.

Oligomerization state of the serotonin$_{1A}$ receptor by pbICS

We previously showed that the heterologously expressed EYFP-tagged serotonin$_{1A}$ receptor in CHO cells is functionally similar to the native receptor.[42] Knowledge of the oligomerization status of the receptor is important since receptor function and signaling could depend on its oligomeric state.[20,47] In this work, our objective was to exploit the dependence of cluster density on photobleaching in ICS to explore the oligomeric status of the serotonin$_{1A}$ receptor and its modulation with membrane cholesterol.

ICS measures cluster density of aggregates in a given region[32,33] and cluster density is inversely proportional to the amplitude of the spatial correlation function. The cluster density reduces upon photobleaching (increases with remaining fluorescence) and the correlation between cluster density and remaining fluorescence intensity depends on the oligomeric state of the fluorophore-tagged receptor. A representative confocal microscopic image of serotonin$_{1A}$-EYFP receptors on the top membrane surface of CHO cells showing predominantly membrane localization of the receptor is shown in Fig. 1a. We selected a 128 × 128 pixel by pixel region of interest (ROI) from the confocal image and subjected it to image correlation analysis (see Fig. 1b). The spatial autocorrelation of the ROI was calculated using ImageJ software and Fig. 1c shows a representative spatial autocorrelation function. The cluster density was calculated from the intercept on the ordinate (y-axis) of the spatial autocorrelation function. Similarly, the cluster density was calculated for stacks of images that were collected upon progressive photobleaching. The cluster density was plotted as a function of fractional remaining fluorescence (Fig. 2a) and the plot was analyzed using eqn (7) to estimate the fraction of various oligomeric states.

A schematic representation of photobleaching probabilities of fluorescing populations of various oligomeric states is shown in Fig. 2b. The dependence of apparent cluster density on remaining fluorescence is shown in Fig. 2c. For monomeric receptors, the amount of fluorescence remaining would be proportional to the number of fluorescent monomers (the remaining fraction being photobleached and thereby not contributing to the observed fluorescence). The apparent cluster density in this case would be a linear function of the fractional remaining fluorescence (see Fig. 2c). For higher order oligomers, a greater number of monomer units of the oligomer need to be photobleached to obtain

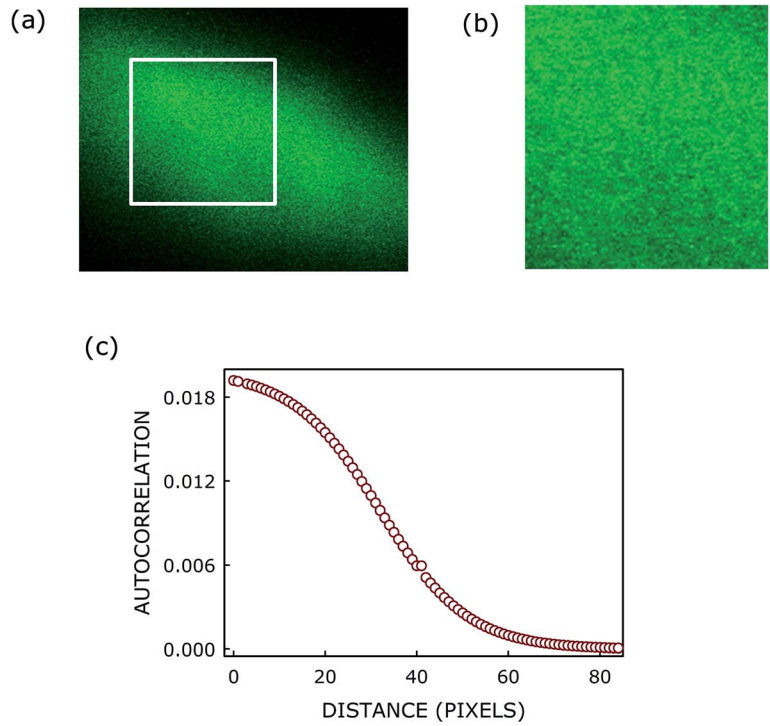

Fig. 1 (a) A representative confocal microscopic image of serotonin$_{1A}$-EYFP receptors on the top membrane surface of CHO cells. (b) A 128 × 128 region of interest (ROI, shown as a box in (a)) was cropped from the image (a) and was subjected to pbICS analysis. (c) Representative spatial autocorrelation for image (b).

complete photobleaching (Fig. 2b). The apparent cluster density, therefore, would exhibit a nonlinear dependence on remaining fluorescence for higher order oligomers (Fig. 2c). The extent of nonlinearity would increase with the increase in size of the oligomeric state.

The cluster density of serotonin$_{1A}$ receptors measured as a function of fractional remaining fluorescence upon photobleaching is shown in Fig. 3a. Data was fitted to eqn (7) to obtain the fraction of various oligomeric states of the receptor. This analysis showed that the serotonin$_{1A}$ receptor exists predominantly as trimers (~60%) with equal contributions from monomeric (~20%) and dimeric (~20%) receptors in control conditions (see Fig. 3b).

Cholesterol-dependent oligomerization state of the serotonin$_{1A}$ receptor

We have previously shown that membrane cholesterol plays a crucial role in the function and organization of the serotonin$_{1A}$ receptor.[43,48–51] Specific agonist binding to the serotonin$_{1A}$ receptor, measured using [^{3}H]8-OH-DPAT, upon modulation of membrane cholesterol, is shown in Fig. 4a. The figure shows that the specific [^{3}H]8-OH-DPAT binding exhibits an increase of ~57% upon depletion of membrane cholesterol using MβCD. MβCD is a water-soluble polymer of methylated-glucose, and has been extensively used to selectively and efficiently

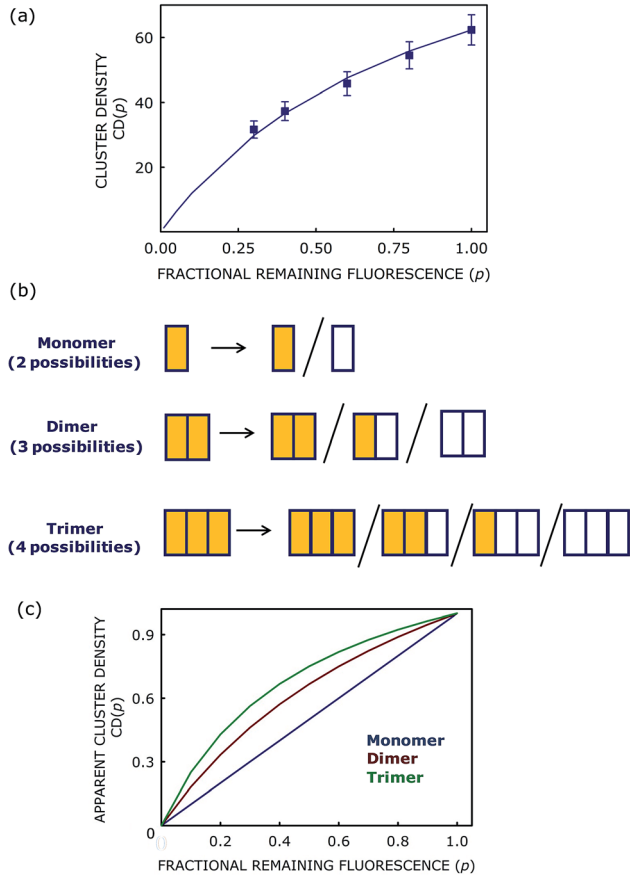

Fig. 2 (a) A representative cluster density plot as a function of remaining fluorescence upon photobleaching of serotonin$_{1A}$-EYFP receptors in CHO cells. Data shown are means ± S.E. of at least six independent measurements. (b) A schematic model illustrating various possibilities of photobleaching of oligomeric states. The arrows indicate photobleaching. (c) Theoretical plots of cluster density as a function of fraction of remaining fluorescence for monomer (blue), dimer (maroon) and trimer (green) states generated using eqn (3)–(5).

extract cholesterol from membranes by incorporating it in a central nonpolar cavity.[52] Interestingly, upon replenishment of membrane cholesterol using MβCD-cholesterol complex, the specific [^{3}H]8-OH-DPAT binding was restored to control level (see Fig. 4a). With an overall goal to address any change in oligomerization pattern accompanying the change in receptor activity due to cholesterol modulation, we carried out pbICS analysis under these conditions (see Fig. 4b).

As mentioned above (Fig. 3b), the serotonin$_{1A}$ receptor exists predominantly as trimers (~60%) with ~20% contribution from both monomeric and dimeric populations under control (normal) membrane cholesterol. The oligomeric distribution of receptors displayed a marked shift upon depletion of membrane cholesterol (see Fig. 4b). Fitting of pbICS data obtained under these conditions to eqn (7) yielded the fraction of various oligomeric states of the receptor. These

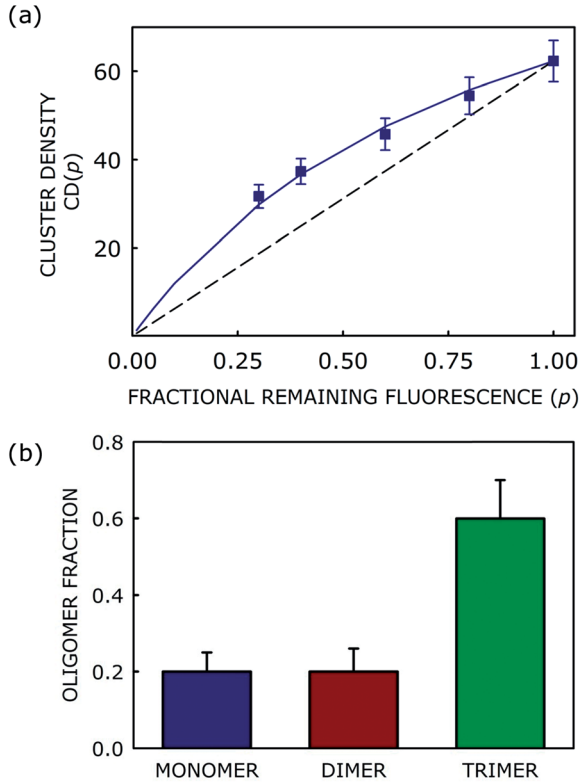

Fig. 3 (a) Cluster density as a function of remaining fractional fluorescence upon photobleaching for serotonin$_{1A}$-EYFP receptors in CHO cells. Data shown are means ± S.E. of at least six independent measurements. Experimental points were fitted to a monomer–dimer–trimer distribution of cluster sizes using eqn (7). A dashed linear line corresponding to the fit to a monomeric distribution of cluster size is shown for comparison. See the Experimental section for more details. (b) Fraction of monomer, dimer and trimer components obtained by fitting the data to a monomer–dimer–trimer distribution model. Data shown are means ± S.E. of at least six independent measurements.

results show that the serotonin$_{1A}$ receptor exists predominantly in the dimeric state (∼95%) under cholesterol-depleted conditions. The population of the momomeric receptor in this condition is ∼5% while the contribution from the trimeric population is negligible (<0.5%). The increase in dimeric receptor population upon cholesterol depletion is in overall agreement with our previous results on receptor oligomerization using photobleaching homo-FRET[20] and coarse-grain molecular dynamics simulations.[23] Upon comparison of Fig. 4a and b, it appears that the dimeric form of the serotonin$_{1A}$ receptor contributes most to ligand binding activity, relative to the monomeric and trimeric forms.

Fig. 4a shows that upon replenishment of membrane cholesterol in cholesterol-depleted cells using MβCD-cholesterol complex, the specific [^{3}H]8-OH-DPAT binding could be restored to control level. To monitor whether the recovery of ligand binding activity was due to change in distribution of oligomeric states of the receptor, we carried out pbICS analysis under this condition. Fig. 4b shows that there is a change in oligomeric distribution of receptors upon

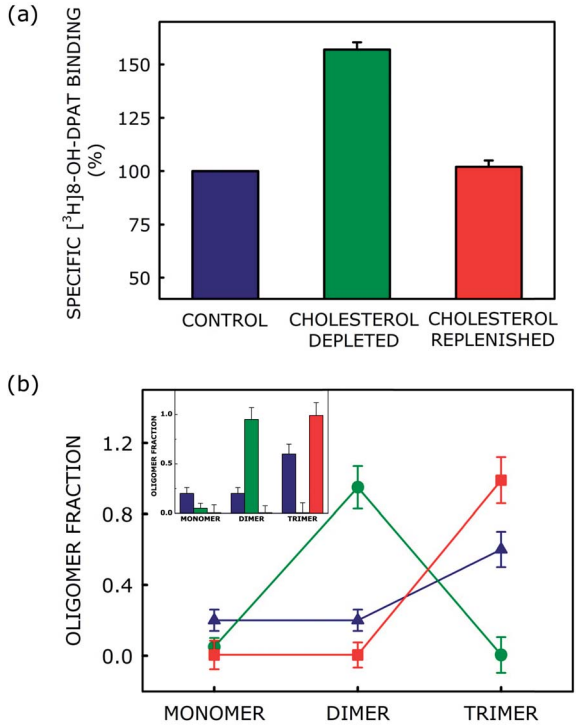

Fig. 4 (a) Specific agonist ([^{3}H]8-OH-DPAT) binding to serotonin$_{1A}$-EYFP receptors in membranes isolated from control, cholesterol-depleted and cholesterol-replenished cells. The results shown are means ± S.E. of at least four independent measurements. (b) Variations of monomer, dimer and trimer components of the serotonin$_{1A}$ receptor under conditions of varying membrane cholesterol content. The fraction of oligomeric components of the receptor in control (▲), cholesterol-depleted (●) and cholesterol-replenished (■) cells is shown. The fractions of different oligomeric states were estimated by fitting cluster density as a function of fractional remaining fluorescence using eqn (7). The results shown are means ± S.E. of at least six independent measurements. Lines joining data points are provided as viewing guides. The inset shows the same data as a bar plot (same color coding: blue: control, green: cholesterol-depleted, red: cholesterol-replenished). See the Experimental section for more details.

cholesterol replenishment. The figure shows that the predominant oligomeric state of the receptor under cholesterol-replenished conditions is trimeric (~99%). The contribution from the other oligomeric states (monomer and dimer) is negligible. The restoration of ligand binding activity to control levels upon replenishment of membrane cholesterol could therefore be attributed to the change in oligomeric state of the receptor. It should be mentioned here that our results show that replenishment of cholesterol using MβCD-cholesterol complex resulted in a cholesterol level which was somewhat higher relative to the control level. We found it experimentally difficult to manipulate conditions in such a way so as to bring back the cholesterol level exactly to control levels (prior to depletion). This could be a possible reason for not obtaining the same proportion of various oligomers in control and cholesterol-replenished conditions, although there is an overall agreement (increase in trimer population).

Discussion

Taken together, we show here that pbICS represents a convenient approach to monitor the oligomeric state of membrane receptors. Our results show that the oligomeric state of the serotonin$_{1A}$ receptor is controlled by cell membrane cholesterol (see Fig. 5). In control conditions, the majority of the receptor population exists as trimers, with equal contributions from monomeric and dimeric receptor populations. The distribution of receptors in various oligomeric states appears to change significantly upon cholesterol depletion. In cholesterol-depleted conditions, the receptor appears to exist predominantly as dimers with minor contributions from the other oligomeric forms. These results, along with the observation that the specific ligand binding activity of the serotonin$_{1A}$ receptor exhibits a considerable increase, suggest that the dimeric population of the receptor could contribute toward ligand binding activity in a major way. These results are supported upon replenishment of cell membrane cholesterol, which results in restoration of ligand binding activity to the control level and a change in the distribution of oligomeric states leading to an increase in trimeric population and a concominant reduction in the dimeric population of receptors.

GPCR oligomerization assumes greater relevance in designing better therapeutic strategies. Importantly, earlier reports have demonstrated the increased specificity of multivalent drugs,[53] as well as ligand sensitivity of the various GPCR oligomer interfaces.[47] We have recently shown that GPCR dimer organization is controlled by membrane cholesterol, and this could have potential implications in cellular physiology and drug discovery.[22,23] Since cellular cholesterol is developmentally regulated and increases with aging,[54,55] oligomeric states of GPCRs could be age-dependent. Correlation of receptor activity with oligomeric states of

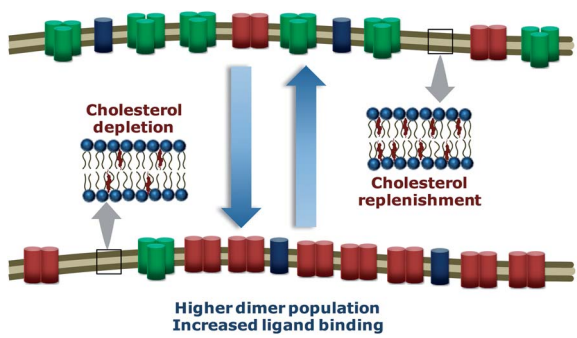

Fig. 5 A schematic model of the oligomeric status of serotonin$_{1A}$ receptors with varying cholesterol content. The model shows an initial heterogeneous oligomeric state of the serotonin$_{1A}$ receptor in control cells. Depletion of membrane cholesterol appears to favor the dimeric state of the serotonin$_{1A}$ receptors and the specific agonist binding to the receptors is higher under these conditions. Upon cholesterol replenishment, the oligomeric state of the receptor changes in such a way that the dimers disappear giving rise predominantly to a trimer population (it is to be noted here that the exact distribution of oligomers is different in control and upon cholesterol replenishment (Fig. 4b); this figure is a schematic and mainly shows the increase in trimer population upon replenishment). These results imply that the receptor dimer is primarily responsible for enhanced agonist binding.

the receptor could therefore lead to a better understanding of GPCR function in health and disease.

Conflict of interest

The authors declare that there is no conflict of interest.

Acknowledgements

This work was supported by the Science and Engineering Research Board (Govt. of India) project (EMR/2016/002294) to A. C. A. H. A. C. acknowledges ARC funding through DP110100164 and DP130101475 grants. A. C. gratefully acknowledges support from J. C. Bose Fellowship (Department of Science and Technology, Govt. of India). H. C. thanks the Council of Scientific and Industrial Research for the award of a Senior Research Associateship and the University Grants Commission for UGC-Assistant Professor position and UGC-Start-Up Grant (F.4-5(138-FRP)/2014(BSR)). A. C. is an Adjunct Professor of Tata Institute of Fundamental Research (Mumbai), Indian Institute of Technology (Kanpur), and Swinburne University of Technology (Melbourne, Australia). We thank G. Aditya Kumar for help in making figures and members of the Chattopadhyay laboratory for their comments and discussions.

References

1 K. L. Pierce, R. T. Premont and R. J. Lefkowitz, *Nat. Rev. Mol. Cell Biol.*, 2002, **3**, 639.
2 D. M. Rosenbaum, S. G. F. Rasmussen and B. K. Kobilka, *Nature*, 2009, **459**, 356.
3 A. Chattopadhyay, *Adv. Biol.*, 2014, **2014**, 143023.
4 K. A. Jacobson, *Biochem. Pharmacol.*, 2015, **98**, 541.
5 R. M. Cooke, A. J. H. Brown, F. H. Marshall and J. S. Mason, *Drug Discovery Today*, 2015, **20**, 1355.
6 T. J. Pucadyil and A. Chattopadhyay, *Prog. Lipid Res.*, 2006, **45**, 295.
7 Y. D. Paila and A. Chattopadhyay, *Subcell. Biochem.*, 2010, **51**, 439.
8 J. Oates and A. Watts, *Curr. Opin. Struct. Biol.*, 2011, **21**, 802.
9 M. Jafurulla and A. Chattopadhyay, *Curr. Med. Chem.*, 2013, **20**, 47.
10 M. Jafurulla and A. Chattopadhyay, *Eur. J. Pharmacol.*, 2015, **763**, 241.
11 G. Gimpl, *Chem. Phys. Lipids*, 2016, **199**, 61.
12 K. Shanti and A. Chattopadhyay, *Curr. Sci.*, 2000, **79**, 402.
13 M. J. Lohse, *Curr. Opin. Pharmacol.*, 2010, **10**, 53.
14 K. Palczewski, *Trends Biochem. Sci.*, 2010, **35**, 595.
15 G. Milligan, *Curr. Opin. Pharmacol.*, 2010, **10**, 23.
16 K. Herrick-Davis, E. Grinde, A. Cowan and J. E. Mazurkiewicz, *Mol. Pharmacol.*, 2013, **84**, 630.
17 S. Terrillon and M. Bouvier, *EMBO Rep.*, 2004, **5**, 30.
18 M. Bellot, S. Galandrin, C. Boularan, H. J. Matthies, F. Despas, C. Denis, J. Javitch, S. Mazères, S. J. Sanni, V. Pons, M.-H. Seguelas, J. L. Hansen, A. Pathak, A. Galli, J.-M. Sénard and C. Galés, *Nat. Chem. Biol.*, 2015, **11**, 271.
19 H. Chakraborty and A. Chattopadhyay, *ACS Chem. Neurosci.*, 2015, **6**, 199.

20 S. Ganguly, A. H. A. Clayton and A. Chattopadhyay, *Biophys. J.*, 2011, **100**, 361.
21 Y. D. Paila, M. Kombrabail, G. Krishnamoorthy and A. Chattopadhyay, *J. Phys. Chem. B*, 2011, **115**, 11439.
22 X. Prasanna, A. Chattopadhyay and D. Sengupta, *Biophys. J.*, 2014, **106**, 1290.
23 X. Prasanna, D. Sengupta and A. Chattopadhyay, *Sci. Rep.*, 2016, **6**, 31858.
24 J. Shan, G. Khelashvili, S. Mondal, E. L. Mehler and H. Weinstein, *PLoS Comput. Biol.*, 2012, **8**, e1002473.
25 S. Mondal, J. M. Johnston, H. Wang, G. Khelashvili, M. Filizola and H. Weinstein, *Sci. Rep.*, 2013, **3**, 2909.
26 K. A. Marino, D. Prada-Gracia, D. Provasi and M. Filizola, *PLoS Comput. Biol.*, 2016, **12**, e1005240.
27 S. Gahbauer and R. A. Böckmann, *Front. Physiol.*, 2016, **7**, 494.
28 A. H. A. Clayton and A. Chattopadhyay, *Biophys. J.*, 2014, **106**, 1227.
29 S. Ferré, V. Casadó, L. A. Devi, M. Filizola, R. Jockers, M. J. Lohse, G. Milligan, J.-P. Pin and X. Guitart, *Pharmacol. Rev.*, 2014, **66**, 413.
30 M. Scarselli, P. Annibale, P. J. McCormick, S. Kolachalam, S. Aringhieri, A. Radenovic, G. U. Corsini and R. Maggio, *FEBS J.*, 2016, **283**, 1197.
31 H. Guo, S. An, R. Ward, Y. Yang, Y. Liu, X.-X. Guo, Q. Hao and T.-R. Xu, *Biosci. Rep.*, 2017, **37**, BSR20160547.
32 N. O. Petersen, P. L. Höddelius, P. W. Wiseman, O. Seger and K.-E. Magnusson, *Biophys. J.*, 1993, **65**, 1135.
33 N. O. Petersen, C. Brown, A. Kaminski, J. Rocheleau, M. Srivastava and P. W. Wiseman, *Faraday Discuss.*, 1998, **111**, 289.
34 P. W. Wiseman and N. O. Petersen, *Biophys. J.*, 1999, **76**, 963.
35 G. D. Ciccotosto, N. Kozer, T. T. Y. Chow, J. W. M. Chon and A. H. A. Clayton, *Biophys. J.*, 2013, **104**, 1056.
36 N. Kozer, D. Barua, S. Orchard, E. C. Nice, A. W. Burgess, W. S. Hlavacek and A. H. A. Clayton, *Mol. BioSyst.*, 2013, **9**, 1849.
37 S. Ganguly and A. Chattopadhyay, *Biophys. J.*, 2010, **99**, 1397.
38 T. J. Pucadyil, S. Kalipatnapu and A. Chattopadhyay, *Cell. Mol. Neurobiol.*, 2005, **25**, 553.
39 C. P. Müller, R. J. Carey, J. P. Huston and M. A. De Souza Silva, *Prog. Neurobiol.*, 2007, **81**, 133.
40 E. Lacivita, M. Leopoldo, F. Berardi and R. Perrone, *Curr. Top. Med. Chem.*, 2008, **8**, 1024.
41 F. Fiorino, B. Severino, E. Magli, A. Ciano, G. Caliendo, V. Santagada, F. Frecentese and E. Perissutti, *J. Med. Chem.*, 2014, **57**, 4407.
42 T. J. Pucadyil, S. Kalipatnapu, K. G. Harikumar, N. Rangaraj, S. S. Karnik and A. Chattopadhyay, *Biochemistry*, 2004, **43**, 15852.
43 T. J. Pucadyil and A. Chattopadhyay, *Biochim. Biophys. Acta*, 2007, **1768**, 655.
44 S. Kalipatnapu, T. J. Pucadyil, K. G. Harikumar and A. Chattopadhyay, *Biosci. Rep.*, 2004, **24**, 101.
45 P. K. Smith, R. I. Krohn, G. T. Hermanson, A. K. Mallia, F. H. Gartner, M. D. Provenzano, E. K. Fujimoto, N. M. Goeke, B. J. Olson and D. C. Klenk, *Anal. Biochem.*, 1985, **150**, 76.
46 D. M. Amundson and M. Zhou, *J. Biochem. Biophys. Methods*, 1999, **38**, 43.
47 F. Mancia, Z. Assur, A. G. Herman, R. Siegel and W. A. Hendrickson, *EMBO Rep.*, 2008, **9**, 363.
48 T. J. Pucadyil and A. Chattopadhyay, *Biochim. Biophys. Acta*, 2004, **1663**, 188.

49 Y. D. Paila, M. R. V. S. Murty, M. Vairamani and A. Chattopadhyay, *Biochim. Biophys. Acta*, 2008, **1778**, 1508.
50 S. Shrivastava, T. J. Pucadyil, Y. D. Paila, S. Ganguly and A. Chattopadhyay, *Biochemistry*, 2010, **49**, 5426.
51 R. Saxena and A. Chattopadhyay, *J. Neurochem.*, 2011, **116**, 726.
52 R. Zidovetzki and I. Levitan, *Biochim. Biophys. Acta*, 2007, **1768**, 1311.
53 A. V. Dix, S. M. Moss, K. Phan, T. Hoppe, S. Paoletta, E. Kozma, Z.-G. Gao, S. R. Durell, K. A. Jacobson and D. H. Appella, *J. Am. Chem. Soc.*, 2014, **136**, 12296.
54 M. Martin, C. G. Dotti and M. D. Ledesma, *Biochim. Biophys. Acta*, 2010, **1801**, 934.
55 K. Smiljanic, T. Vanmierlo, A. M. Djordjevic, M. Perovic, N. Loncarevic-Vasiljkovic, V. Tesic, L. Rakic, S. Ruzdijic, D. Lutjohann and S. Kanazir, *Lipids*, 2013, **48**, 1069.